

748

748

SANDIA REPORT SAND81-1664 • Unlimited Release • UC-70
Printed February 1982

Effects of Elevated Temperature and Pore Pressure on the Mechanical Behavior of Bullfrog Tuff

William A. Olsson

Prepared by
Sandia National Laboratories
Albuquerque, New Mexico 87185 and Livermore, California 94550
for the United States Department of Energy
under Contract DE-AC04-76DP00789



Issued by Sandia National Laboratories, operated for the United States Department of Energy by Sandia Corporation.

NOTICE: This report was prepared as an account of work sponsored by an agency of the United States Government. Neither the United States Government nor any agency thereof, nor any of their employees, nor any of their contractors, subcontractors, or their employees, makes any warranty, express or implied, or assumes any legal liability or responsibility for the accuracy, completeness, or usefulness of any information, apparatus, product, or process disclosed, or represents that its use would not infringe privately owned rights. Reference herein to any specific commercial product, process, or service by trade name, trademark, manufacturer, or otherwise, does not necessarily constitute or imply its endorsement, recommendation, or favoring by the United States Government, any agency thereof or any of their contractors or subcontractors. The views and opinions expressed herein do not necessarily state or reflect those of the United States Government, any agency thereof or any of their contractors or subcontractors.

Printed in the United States of America
Available from
National Technical Information Service
U.S. Department of Commerce
5235 Port Royal Road
Springfield, VA 22161

NTIS price codes
Printed copy: A02
Microfiche copy: A01

SAND81-1664
Unlimited Release

Effects of Elevated Temperature and Pore Pressure on
the Mechanical Behavior of Bullfrog Tuff*

William A. Olsson
Geomechanics Division 5532
Sandia National Laboratories**
Albuquerque, New Mexico 87185

ABSTRACT

Samples of the Bullfrog Member of the Crater Flat Tuff from the depth interval 758.9 to 759.2 m in hole USW-G1 on the Nevada Test Site were tested in triaxial compression. Test conditions were: 1) effective confining pressure to 20 MPa; 2) temperature of 200°C; 3) both dry and with pore water pressures from 3.4 to 5 MPa; and 4) a strain-rate of 10^{-4} /s. The results suggest that the presence of water causes the strength to decrease. In addition, the brittle-ductile transition pressure for this rock was found to be about 15 MPa, regardless of saturation. Below this pressure deformation is characterized by unstable stress drops and the development of a single fracture, and above this pressure deformation is stable and distributed more uniformly throughout the sample.

* This work was supported by the U. S. Department of Energy (DOE) under Contract DE-AC04-76-DPO0789.

** A U. S. DOE Facility.

TABLE OF CONTENTS

	<u>Page</u>
INTRODUCTION	5
RESULTS	6
DISCUSSION	7
CONCLUSIONS	9
REFERENCES	10
FIGURES	12-14

SAND81-1664
Unlimited Release

Effects of Elevated Temperature and Pore Pressure on
the Mechanical Behavior of Bullfrog Tuff

William A. Olsson
Geomechanics Division 5532
Sandia National Laboratories
Albuquerque, New Mexico 87185

INTRODUCTION

The Nevada Nuclear Waste Storage Investigations (NNWSI) project which is administered by the Nevada Operations Office of the U. S. Department of Energy is assessing the feasibility of emplacing nuclear waste in silicic tuffs at Yucca Mountain, on and near the Nevada Test Site. Part of this program consists of design calculations for an underground nuclear-waste repository which require extensive mechanical-property data. A preliminary testing program (Olsson and Jones, 1980) concentrated on nominally dry samples at room temperature. The rock near a proposed repository at depths below the water table is wet, and will be subjected to both thermal and mechanical loading, so it is necessary to determine the effects of these variables on matrix mechanical properties. Accordingly, samples of the Bullfrog Member of the Crater Flat Tuff from the depth interval 758.9 to 759.2 in hole USW-G1 on the NTS were tested in triaxial compression at test conditions of: 1) effective confining pressure to 20 MPa; 2) temperature of 200°C; 3) sample state both dry and with pore water pressures from 3.4 to 5 MPa; and 4) a strain-rate of 10^{-4} /s.

Because sample availability was limited, it was necessary to recore test specimens 2.54 cm in diameter and 5.08 cm long from a 6.3 cm-diameter sample core. Seven specimens were recovered. The small size of the specimens precluded specimen volume measurement during the triaxial tests because the sensitivity of the dilatometric volume-measuring system is not sufficient. Thus, only axial load-deformation data were measured.

Specimens were jacketed with sleeves of silicone rubber sealant. Constant pore pressure was applied to both ends of the samples. The calculated porosity of tuff at a depth of 759.9 m is 0.27; this is probably representative of the rock tested.

RESULTS

Four of the seven samples were tested dry and vented at 200°C. Effective confining pressures were 5, 10, and 20 MPa. Stress-strain curves for these tests are shown in Figure 1. Curves obtained at the two lower confining pressures exhibit maximums in the stress difference, followed by intervals of decreasing stress; eventually the stress becomes essentially constant. The peak stress is taken to indicate the fracture stress, and the lower value of stress at high strain is a measure of the frictional resistance to sliding on shear fractures formed during the falling part of the stress-strain curves. The 10-MPa test illustrates this shape best; the 5-MPa test had not yet reached a constant value of stress. The two tests run at 20 MPa show little or no stress-drop after peak stress, although the curve for sample number 5 shows a sudden decrease in stress at 2.8% strain, which was caused by a leak in the jacket.

Posttest examination of the specimens show that, at 5 MPa effective confining pressure, this tuff develops a well-defined but irregular shear fracture at about 25° to the axis of maximum compression. At 20 MPa,

deformation is distributed over numerous intersecting shear fractures, causing the specimen to take on a bulging appearance. At 10 MPa, the macroscopic mode of deformation is intermediate between those at higher and lower confining pressures. The strength of the dry specimens increases from 87 MPa at 5 MPa confining pressure to an average of 134 MPa at 20.7 MPa confining pressure (Table 1).

The results for the three tests run with constant pore pressure are exhibited in Figure 2. A trend similar to that for the dry specimens is seen with regard to the shape of the stress-strain curve as a function of confining pressure. That is, at 5 MPa effective confining pressure, there is a well-defined stress maximum which is followed by a stress drop and a subsequent interval of constant stress. At 12.5 MPa, the stress drop is more gradual, and occurs at a higher strain. There is no stress drop at 20 MPa. The macroscopic modes of deformation are the same as for the dry specimens. The strength of the wet specimens (Table 1) increases from 70 MPa at an effective confining pressure of 5 MPa to 86 MPa at an effective confining pressure of 20.7 MPa.

DISCUSSION

Orowan (1960) suggested that the gradual disappearance of post-fracture stress drops with increased confining pressure can be explained in terms of the relative values of the frictional resistance to sliding and the shear strength of intact rock. At lower pressures, the frictional resistance to sliding is less than the matrix shear-fracture stress, so that when the shear fracture forms, stress drops to an equilibrium value dictated by the sliding resistance (e.g., the 5 MPa and 10 MPa curves in Figure 1). Because frictional resistance to sliding increases more rapidly with confining pressure than does intact rock strength (e.g., Olsson, 1973), there comes a point when the fracture stress and frictional

stress are equal. Deformation will then be distributed more uniformly throughout the specimen, and it may occur as either distinct shear fractures or as a more ductile mode of deformation characterized by crystal plasticity.

The pressure at which the disappearance of post-fracture stress drops is essentially complete has been referred to as the brittle-ductile transition pressure (Heard, 1960; Byerlee, 1968). Examples comparing friction stress as a function of confining pressure to intact rock shear strength as a function of confining pressure for different rock types may be found in Byerlee (1968) and Olsson (1973).

It is clear from the macroscopic modes of deformation and shapes of the stress-strain curves that Bullfrog tuff (0.27 porosity) deformed at 200°C, wet or dry, is characterized by a brittle-ductile transition at the relatively low effective confining pressure of about 15 MPa. There are at least two implications of this behavior: the first is related to excavation stability and the second concerns altered permeability. With regard to the first point the specimens were tested in a displacement-controlled machine, so that no increase in strain-rate occurred during fracturing. In loading systems that have higher effective compliances, such as the in-situ loading system which is comprised of the surrounding rock plus discontinuities and voids, such stress drops can take place much more rapidly. In fact, seismic energy can be released, or structural integrity lost. Thus, the higher the effective confining pressure, the less likely structural instability is to occur as a result of postfracture stress drops.

As to the second implication of altered permeability, at low confining pressure where failure occurs along one well-defined fracture, permeability will be enhanced due to the presence of the fracture. However, at a pressure at which many fractures are formed throughout the specimen, permeability may be enhanced even more. Alternatively, permeability may

change little if the multiple fractures are not interconnected. Extrapolation to the field, however, also requires consideration of the competing process of decreased fracture permeability due to increased pressure.

The effect of the presence of water on the strength of the Bullfrog samples studied here is shown in Figure 3 as a plot of $\sqrt{J_2} = (\sigma_1 - \sigma_3)/\sqrt{3}$ against $I_1/3 - P_p$. J_2 is the second invariant of the stress deviator, I_1 is the first stress invariant, and P_p is the pore pressure. A straight-line fit, calculated by the method of least squares, is drawn through the dry data points as a reference. There are insufficient data from saturated tests to establish an accurate relationship between shear strength and mean effective pressure, but the trend is clear: the presence of water has a significant weakening effect. This is consistent with earlier findings at room temperature on welded samples from the Grouse Canyon Member of the Belted Range Tuff (Olsson and Jones, 1980).

CONCLUSIONS

The seven tests reported here are consistent with the following conclusions:

1. The presence of water causes the strength of welded tuff to decrease, at least at a temperature of 200°C.
2. The brittle-ductile transition pressure for Bullfrog tuff with a porosity near 0.27 is about 15 MPa, regardless of saturation state; the dependence of this pressure upon strain rate remains undefined.
3. Below the brittle-ductile transition pressure, postfracture deformation is characterized by unstable stress drops; at higher pressures, postfracture deformation is stable.

REFERENCES

- Byerlee, J. D., "Brittle-Ductile Transition in Rocks," J. Geophys. Res., Vol. 73, pp. 4741-4750, 1980.
- Heard, H. C., "Transition from Brittle Fracture to Ductile Flow in Solenhofen Limestone as a Function of Temperature, Confining Pressure, and Interstitial Fluid Pressure," in Rock Deformation, D. Griggs and J. Handin, eds., Geol. Soc. Am. Memoir 79, pp. 193-226, 1960.
- Olsson, W. A., "Effects of Temperature, Pressure and Displacement Rate on the Frictional Characteristics of a Limestone," Int. J. Rock Mech. Min. Sci., Vol. 11, pp. 267-278, 1973.
- Olsson, W. A. and Jones, A. K., "Rock Mechanics Properties of Volcanic Tuffs from the Nevada Test Site," Sandia National Laboratories Report, SAND80-1453, Sandia National Laboratories, Albuquerque, NM, November 1980.
- Orowan, E., "Mechanism of Seismic Faulting," in Rock Deformation, D. Griggs and J. Handin, eds., Geol. Soc. Am. Memoir 79, pp. 323-345, 1960.

Table 1. Triaxial Test Data for Bullfrog Tuff at 200°C

<u>Sample Number</u>	<u>Confining Pressure (MPa)</u>	<u>Pore Pressure (MPa)</u>	<u>Maximum Differential Stress (MPa)</u>	<u>Young's Modulus (GPa)</u>
3	5	0	87	16.5
4	10	0	93	15.7
2	20.7	0	119	17.6
5	20.7	0	148	20.5
7	10	5	70	13.1
6	17.5	5	83	17.8
1	24.1	3.4	86	13.8

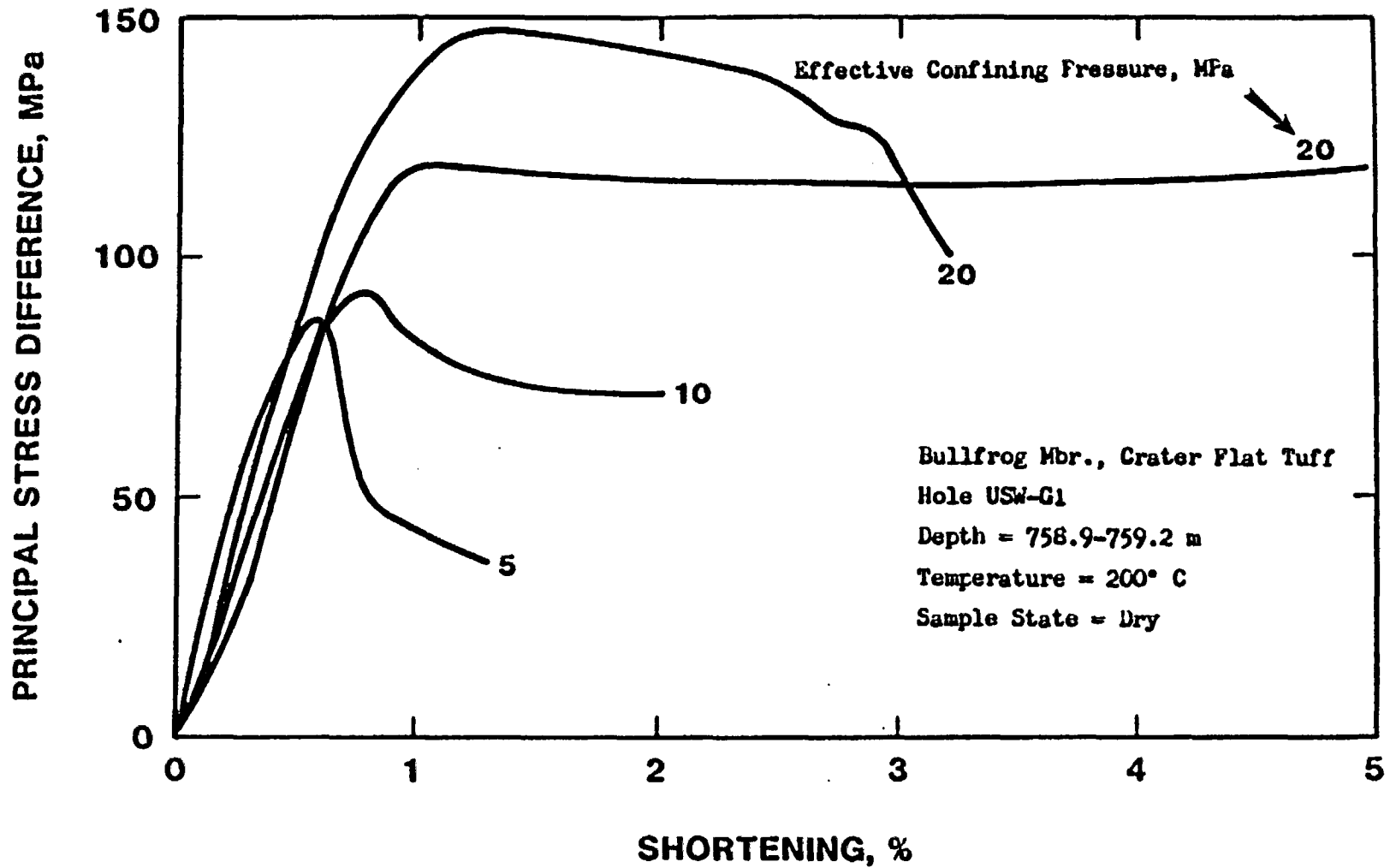


Figure 1: Stress-strain curves for Bullfrog tuff obtained on dry samples at 200°C.

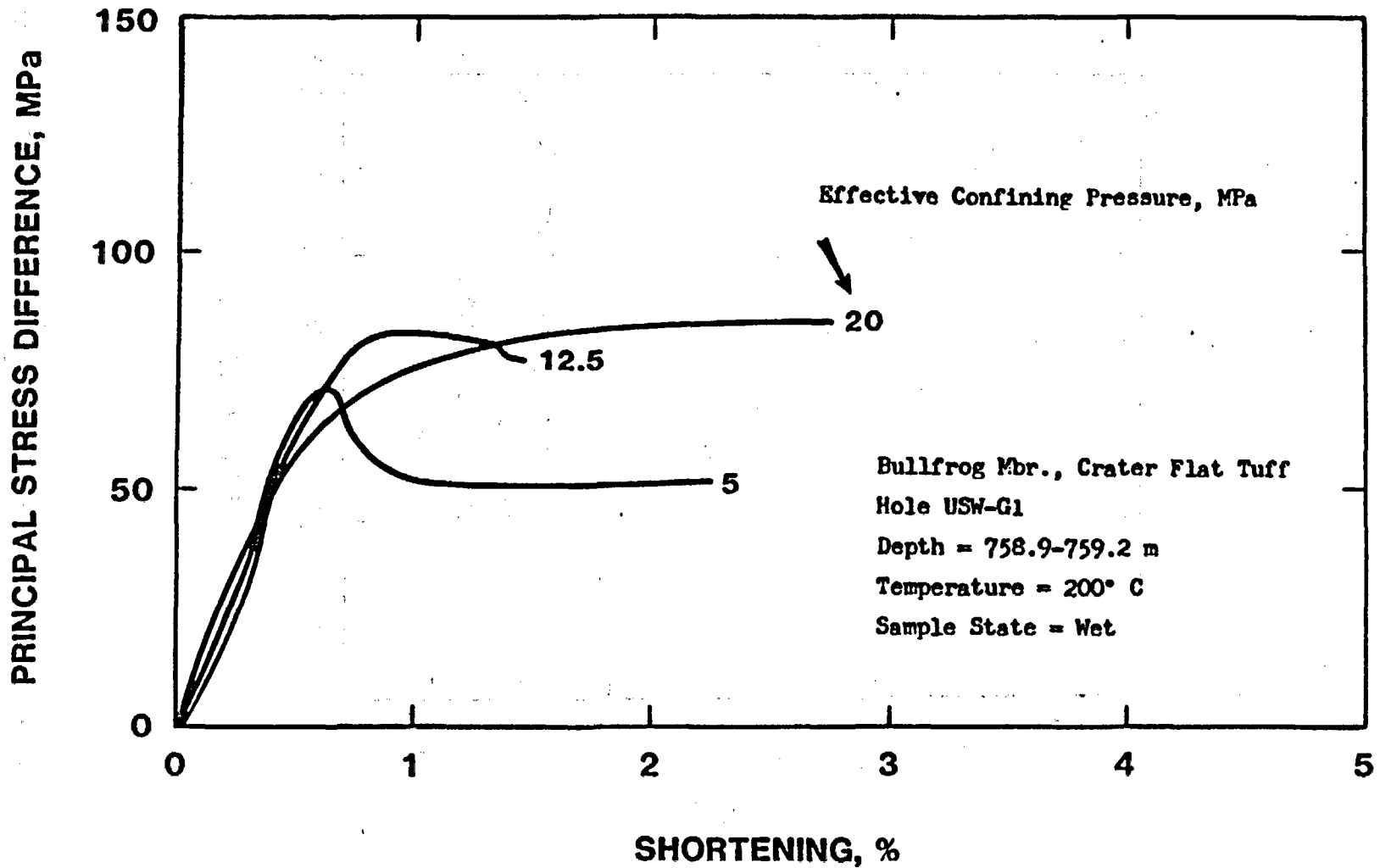


Figure 2: Stress-strain curves for Bullfrog tuff obtained on wet samples with constant pore pressure at 200°C.

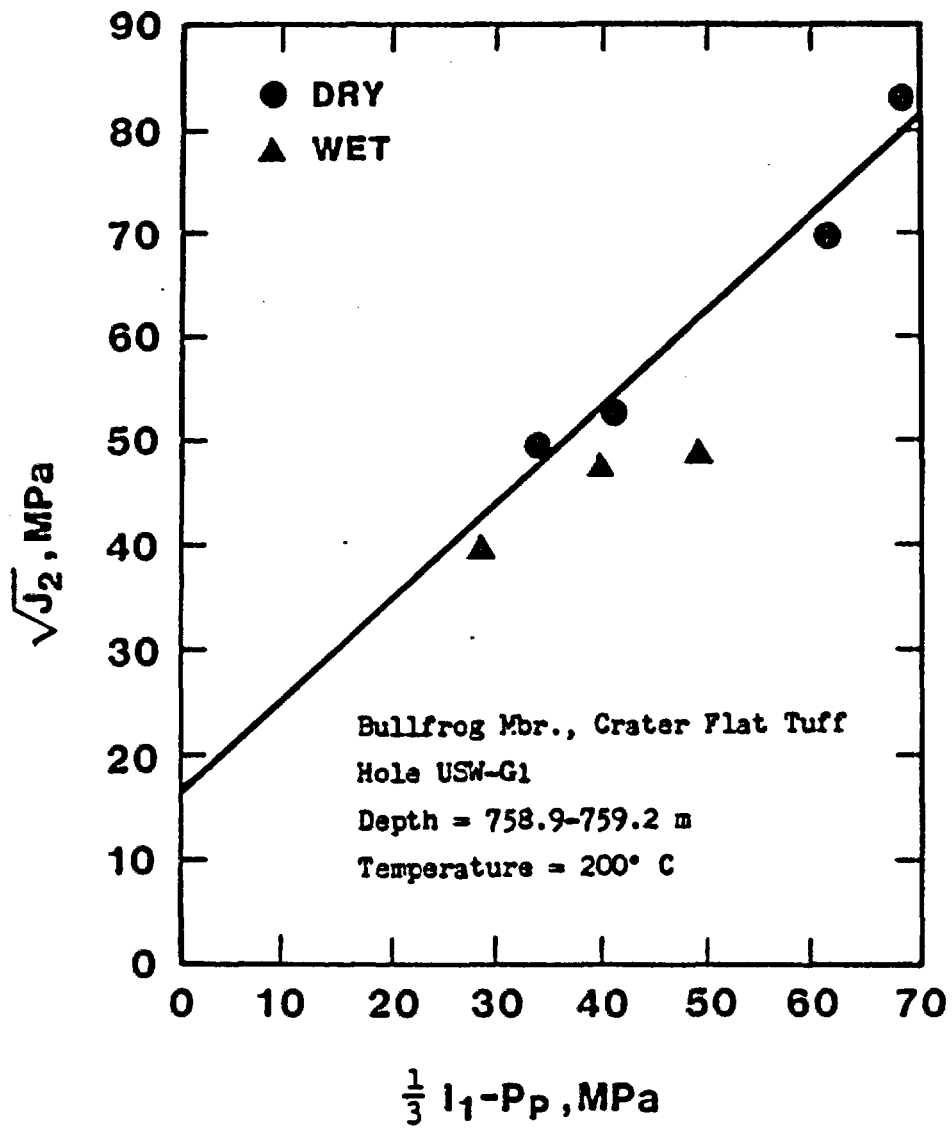


Figure 3: Shear strength-mean effective pressure relationship for Bullfrog tuff at 200°C, both wet and dry.

Distribution:

C. A. Heath, Director
Office of Waste Isolation
U. S. Department of Energy
Room B-207
Germantown, MD 20767

D. L. Vieth, Acting Team Leader
Technology Team
U. S. Department of Energy
Room B-220
Germantown, MD 20767

J. O. Neff, Program Manager
National Waste Terminal
Storage Program Office
U. S. Department of Energy
505 King Avenue
Columbus, OH 43201

L. D. Ramspott
Technical Project Officer
Lawrence Livermore National
Laboratory
University of California
P. O. Box 808
Mail Stop L-204
Livermore, CA 94550

B. R. Erdal
Technical Project Officer
Los Alamos National Laboratory
University of California
P. O. Box 1663
Mail Stop 514
Los Alamos, NM 87545

A. R. Hahl, Site Manager
Westinghouse - AESD
P. O. Box 708
Mail Stop 703
Mercury, NV 89023

G. L. Dixon
Technical Project Officer
U. S. Geological Survey
P. O. Box 25046
Mail Stop 954
Federal Center
Denver, CO 80301

W. E. Wilson
U. S. Geological Survey
P. O. Box 25046
Mail Stop 954
Denver, CO 80301

W. S. Twenhofel
820 Estes Street
Lakewood, CO 80226

C. R. Cooley, Deputy Director
Office of Waste Isolation
U. S. Department of Energy
Room B-214
Germantown, MD 20767

R. G. Goranson
U. S. Department of Energy
Richland Operations Office
P. O. Box 550
Richland, WA 99352

R. Deju
Rockwell International Atomic
International Division
Rockwell Hanford Operations
Richland, WA 99352

R. M. Nelson, Jr., Dir. (3)
Waste Management Project Office
U. S. Department of Energy
P. O. Box 14100
Las Vegas, NV 89114

D. F. Miller, Director
Office of Public Affairs
U. S. Department of Energy
P. O. Box 14100
Las Vegas, NV 89114

R. H. Marks
U. S. Department of Energy
CP-1, M/S 210
P. O. Box 14100
Las Vegas, NV 89114

B. W. Church, Director
Health Physics Division
U. S. Department of Energy
P. O. Box 14100
Las Vegas, NV 89114

R. R. Loux (7)
U. S. Department of Energy
P. O. Box 14100
Las Vegas, NV 89114

A. E. Gurrola
Holmes & Narver, Inc.
P. O. Box 14340
Las Vegas, NV 89114

K. Street, Jr.
Lawrence Livermore National
Laboratory
University of California
Mail Stop L-209
P. O. Box 808
Livermore, CA 94550

D. C. Hoffman
Los Alamos National Laboratory
Mail Stop 760
P. O. Box 1663
Los Alamos, NM 87545

N. E. Carter
Battelle
Office of Nuclear Waste Isolation
505 King Avenue
Columbus, OH 43201

W. A. Carbiener
Battelle
Office of IWTS Integration
505 King Avenue
Columbus, OH 43201

S. Goldsmith
Battelle
Office of Nuclear Waste Isolation
505 King Avenue
Columbus, OH 43201

ONWI Library (5)
Battelle
Office of Nuclear Waste Isolation
505 King Avenue
Columbus, OH 43201

R. M. Hill
State Planning Coordinator
Governor's Office of Planning
Coordination
State of Nevada
Capitol Complex
Carson City, NV 89023

N. A. Clark
Department of Energy
State of Nevada
Capitol Complex
Carson City, NV 89710

J. P. Colton
International Atomic Energy
Agency
Div. of Nuclear Power &
Reactors
P. O. Box 590, A-1011
Vienna, Austria

H. D. Cunningham
Reynolds Electrical &
Engineering Company, Inc.
Mail Stop 555
P. O. Box 14400
Las Vegas, NV 89114

J. A. Cross
Fenix & Scisson, Inc.
P. O. Box 15408
Las Vegas, NV 89114

A. M. Friedman
Argonne National Laboratories
9700 S. Cass Avenue
Argonne, IL 60439

A. J. Rothman (2)
Lawrence Livermore National Lab.
University of California
P. O. Box 808, MS L-204
Livermore, CA 94550

1417 F. W. Muller
3141 L. J. Erickson (5)
3151 W. L. Garner (3)
3154-3 C. H. Dalin (25) (For DOE/TIC)
4530 R. W. Lynch
4531 L. W. Scully
4537 L. D. Tyler
4537 B. S. Langkopf
4537 A. R. Lappin
4537 R. M. Zimmerman
4537 R. Shaw
4538 R. C. Lincoln
5500 O. E. Jonas
5510 D. B. Hayes
5511 D. K. Gartling
5520 T. B. Lane
5521 R. K. Thomas
5522 R. L. Johnson

5530 W. Herrmann
5531 M. L. Blanford
5532 B. M. Butcher
5532 D. J. Holcomb
5532 R. H. Price
5532 L. W. Teufel
5532 W. A. Olsson (10)
5533 A. J. Chabai
5533 W. T. Brown
5534 J. R. Asay
5541 W. C. Luth
8214 M. A. Pound

